Elements of Non-Linear Hamiltonian Dynamics

2013 J. Phys.: Conf. Ser. 465 012016

(http://iopscience.iop.org/1742-6596/465/1/012016)

Journal of Physics: Conference Series **465** (2013) 012016 doi:10.1088/1742-6596/465/1/012016

Elements of Non-Linear Hamiltonian Dynamics

R Egydio de Carvalho

Universidade Estadual Paulista-UNESP, 13506-900 Rio Claro, SP–Brazil

e-mail: regydio@rc.unesp.br

Abstract. In this paper we present a set of generic results on Hamiltonian non-linear dynamics. We show the necessary conditions for a Hamiltonian system to present a non-twist scenario and from that we introduce the isochronous resonances. The generality of these resonances is shown from the Hamiltonian given by the Birkhof-Gustavson normal form, which can be considered a toy model, and from an optic system governed by the non-linear map of the annular billiard. We also define a special kind of transport barrier called robust torus. The meanders and shearless curves are also presented and we show the most robust shearless barrier associated with the rotation numbers.

Keywords: isochronous resonances, robust torus, meandering tori, shearless curves.

1. Introduction

Homoclinic chaos, as is known chaos in Hamiltonian systems, is theoretically supported by the as well-known KAM theory [1] and by the Poincaré-Birkhoff theorem [2]. Roughly speaking, KAM theory establishes that a dynamical system of two degrees of freedom governed by a Hamiltonian of the form,

$$H(J_k,\theta_k) = H_0(J_k) + \varepsilon H_1(J_k,\theta_k) \quad ; \quad k=1 \text{ and } 2 \tag{1}$$

which is integrable for $\epsilon = 0$, still has many invariant tori even if $\epsilon \neq 0$, but ϵ small enough.

The simplest version of the theorem associated with the KAM theory, implies that the Hamiltonian must be sufficiently smooth, and the unperturbed Hamiltonian H_0 to be nonsingular, this is it must satisfy the non-degeneracy, or twist, condition [3], $\det\left|\frac{\partial \dot{\theta}_k}{\partial J_j}\right| \neq 0$, where $\dot{\theta}_k = \frac{\partial H_0(\underline{J})}{\partial J_k} = \omega_k$, are the unperturbed frequencies. It means that the rotation number $\rho = \frac{\omega_1}{\omega_2}$ is a monotonically increasing, or decreasing, function. If ρ is a rational number, it defines a rational or resonant torus and similarly it defines an irrational torus when ρ is irrational. When the perturbation is turned on it acts on a resonant torus and as it becomes stronger the neighbourhood of this torus is also affected defining a

resonance region. Typically, this resonance region is constituted by island chains formed by an even number of periodic orbits, which has been continued from the unperturbed system, libration and rotation tori, deformed irrational tori and chaotic orbits. These periodic orbits have alternating stability and the corresponding island chains are called Poincaré–Birkhoff chains.

However, if the rotation number presents an extreme, the non-twist scenario is established and we observe the birth of isochronous resonances [4], which correspond to simultaneous resonances of same period, and new phenomena, not foreseen by the Poincaré's theorem, appear. A new one very important is the occurrence of heteroclinic reconnections among manifolds of hyperbolic fixed points of different isochronous resonances [5]. The new structures that locally appear in the phase space are associated with the possible values of the non-monotonic behaviour of the rotation number. It is important to point out that there is an extension of the KAM theorem, for discrete equations, for non-twist dynamics [6].

2. Resonant Normal Form and the Isochronous Resonances

In order to introduce the isochronous resonances we will consider the toy model, Resonant Normal Form (RNF) [7,8], for an autonomous system with two degrees of freedom described in angle-action variables (J,θ). The RNF is a Hamiltonian function that consists of an expansion series in all variables around an elliptic fixed point. The terms that do not contain the variables angle are grouped and define what we call unperturbed Hamiltonian H_0 (J_1,J_2). The terms containing only the angle θ_1, besides the actions, define the first perturbation H_1 (J_1,J_2,θ_1), which is an integrable perturbation. The non-integrability of the system is only obtained when both angles appear in the total Hamiltonian. So, the Hamiltonian function can be given by,

$$H(J_1, J_2, \theta_1) = \sum_{k=0}^{n} a_k \, J^k + \varepsilon \, f(J_1, J_2)\cos(r\,\theta_1) \quad , \text{ with } \quad a_0 = J_2 \tag{2}$$

where $H_0(J_1, J_2) = \sum_{k=0}^{n} a_k \, J^k$ and f(J_1,J_2) is an analytic and continuous function. The resonance condition is:

$$\left(\dot{\theta}_1\right)_0 = \text{a polynomial of order } (n-1) \text{ in } J_1 = \frac{\partial H_0}{\partial J_1} = 0 \tag{3}$$

and defines (n-1) Isochronous Resonances, each one at each root of this polynomial. The equations of motion are

$$\dot{J}_1 = r\,\varepsilon\, f(J_1, J_2)\, \sin(r\theta_1) \quad , \quad \dot{\theta}_1 = H_0'(J_1, J_2) + \varepsilon\, f'(J_1, J_2)\cos(r\theta_1) \tag{4}$$

and for,

$$\theta_1 = \frac{k\,\pi}{r} \;\Rightarrow\; k = 0, \ldots, 2r-1 \tag{5}$$

we have 2r fixed points located at values of J_1 satisfying

$$H_0'(J_1, J_2) + (-1)^k \, \varepsilon \, f'(J_1, J_2) = 0 \tag{6}$$

The stability distribution of fixed points, in general, depends on the function f (J). If J_i and J_{i+1} are two consecutive roots of the equation above, then if,
f (Ji) f (J_{i+1}) > 0 ➔ defocalized chains ➔ type 1, f (Ji) f (J_{i+1}) < 0 ➔ focalized chains ➔ type 2, and the corresponding scenarios can be visualized according to picture of Figure (1) [9]. Figure (1) is a permitted reproduction of the original work: Voyatzis G, Meletlidou E and Ichtiaroglou S 2002 Chaos, Solitons & Fractals **14** 1179, authorized by Elsevier through the License Number: 3124200437200.

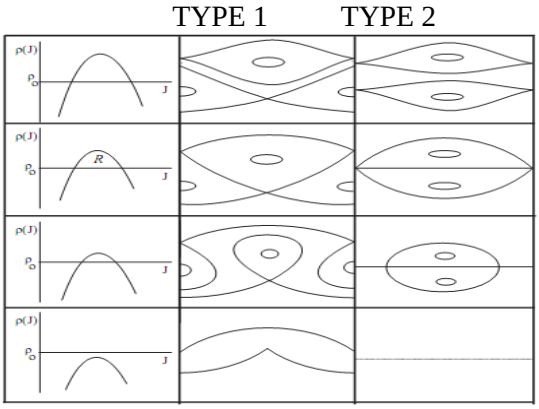

Figure 1: Scheme of the both scenarios with the fixed point aligned or defocused.

In order to present a numerical illustration of the occurrence of isochronous resonances, we have adjusted as the unperturbed Hamiltonian H_0 as the function f (J_1,J_2) and we got,

$$H = \left\{ \left[J_2 - \frac{a}{2}(4J_1 - c)^2 + \frac{1}{4}(4J_1 - c)^4 \right] + \alpha \left\{ \left[b(4J_1 - c)^2 - a \right](4 J_1^2)(J_2 - J_1)^{1/2} \cos(\theta_1) \right\} \right\} \quad (7)$$

where a, b, c, α are adjustable parameters and the action J_2 is a constant of motion since θ_2 is a cyclic variable. Since H_0 is of fourth order in J_1, from equation (2) we identify the position of the three isochronous resonances in the phase space (J_1,θ_1), their positions are

$$(J_1)_+ = \frac{c + \sqrt{a}}{4} \quad , \quad (J_1)_m = \frac{c}{4} \quad , \quad (J_1)_- = \frac{c - \sqrt{a}}{4} \quad (8)$$

where "m" stands for the middle resonance, while "+" the upper resonance and "-" the lower one. In the plots of figure (2) below we observe the three island chains of isochronous resonances for four different values of the perturbation parameter α.

The appearance of resonance chains of same order is the signature of non-twist systems. Besides this effect, the integrable scenario propitiated by the Hamiltonian (7) allows us to observe in a clearer way, in figure (2), the mechanism of the overlap of resonances [10]. As we increase α, the separatrix move toward each other and the overlap starts with a topological rearrangement of the resonance structures. It is worth mentioning that outside this region of isochronous resonances the system behaves as a twist one. The plots of figure (2) are permitted reproduction of the original work: Egydio de Carvalho R, Martins C G L and Favaro G M 2009 Braz. J. Phys.**39** 606, authorized by the Brazilian Physics Society.

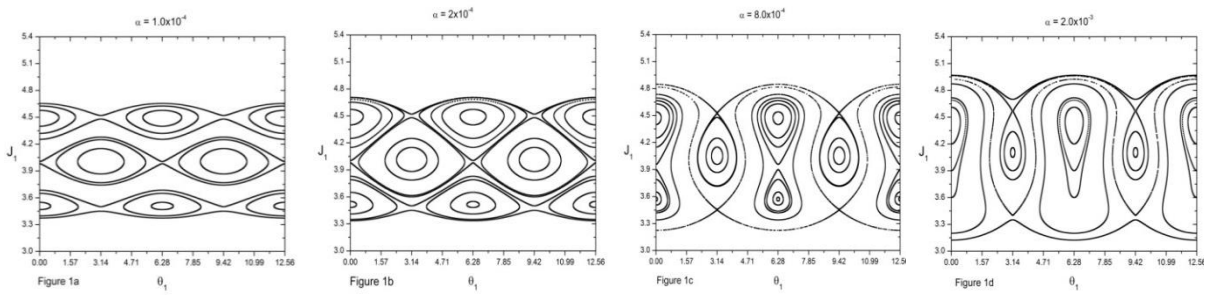

Figure 2: A numerical example of overlap of isochronous resonances in a globally integrable context.

3. The dynamical barrier robust torus

If the function f (J_1,J_2) of the Hamiltonian (2) is a polynomial in J_1 with real roots, then in each root, the perturbation will be algebraically zero. So, invariant curves of H_0 will continue in the perturbed system and we call them by Robust Tori (RT) [3,11].

In the Hamiltonian (7) we identify this function f (J_1,J_2) as,

$$f\,(J_1, J_2) = \left[b\,(4J_1 - c)^2 - a\right](4J_1{}^2)\,(J_2 - J_1)^{1/2} \tag{9}$$

This pre-factor may be null in three different cases: i) $J_1 = 0$, which corresponds to the elliptic point of the system around of which the normal form has been expended and do not add any new information; ii) $J_2 = J_1$, but this case is avoided because numerically we take $J_2 >> J_1$; and iii) $J_1 = \dfrac{c \pm \sqrt{a}}{4}$, which defines two RT in the phase space of the total Hamiltonian.

If the RT are intercalated with the isochronous resonance chains then we obtain the scenario type 2 cited above. On the other hand, if they are external to the chains, we obtain the scenario type 1. Both cases can be seen in figure (3) using the Hamiltonian (7) [11]. The plots of figure (3) are permitted reproduction of the original work: Egydio de Carvalho R and Favaro G M 2005 **350** 173, authorized by Elsevier through the License Number: 3172610159127.

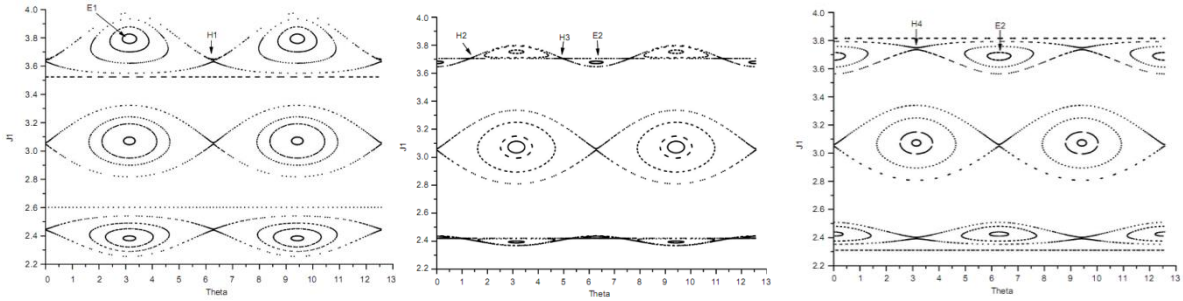

Figure 3: Interaction between the robust tori with the aligned island chains and the defocused scenario.

The movement of the RT from the intercalated to outside configurations is controlled by the parameter b and the mechanism that drives this transition is the successive bifurcation that occur when the RT interact with the separatrix of the islands. The letters H and E in figure (3) corresponds to hyperbolic and elliptic fixed points respectively. A remarkable effect of the presence of the RT is the transition from the focused scenario, where we can observe an alignment of the fixed points of same stability, to defocused scenario or vice-versa.

Since the RT can survive to any generic perturbation that has a polynomial pre-factor, with real roots then, in these situations, they constitute dynamical barriers that separate the phase space in different regions. The existence of this kind of transport barrier can play an important role in different branches of the science, particularly to confinement of plasma in tokamaks [12].

4. Meanders and shearless curves

The isochronous resonances can interact and go into overlapping producing a local, but wide, topological rearrangement. After the overlap, a region with meandering tori appears in the phase space. This kind of tori also corresponds to transport barriers for the dynamics in the phase space. They behave differently under the action of a generic perturbation and their robustness is associated with their rotation number. The destruction of each meandering torus transforms its neighbourhood in a stickiness beach and the last meandering torus to be destroyed is called shearless torus [13,14]. The authors of [14] have shown numerically that other overlap can locally occur inside each meandering region and they called this kind of overlap as second-order reconnection. Other reconnections can happen in smaller scales, inside the meander structures, and thus the order of the reconnections can also increases. After the destruction of the shearless torus a strong stickiness zone emerges. This

region still plays an important role to the dynamics, because it defines local transport barriers [14,15,16,17].

We illustrate the appearance and the robustness of the meandering tori from the labyrinthic standard map non-twist map introduced in [18],

$$x_{n+1} = x_n + a\,(1 - y_{n+1}{}^2) \quad , \quad y_{n+1} = y_n - b\left\{ \sin(2\pi x_n) + \sin(\eta\, 2\pi x_n) \right\} \qquad (10)$$

where a, b and η are adjustable parameters. A remarkable effect is produced through the variation of η. If η = 0 or 1, the system present two isochronous island chains with a pair of fixed points, one being elliptic and the other hyperbolic. Nevertheless, for any other integer η > 1 there occur bifurcations of these fixed points and will exist so many pairs of fixed points as the value of η in each island chain. In figure (4) we present the case for η = 4, in which we can observe four elliptic fixed points as well the four hyperbolic ones in both chains. In all plots from this map we used a = 1.006. The pink lines correspond to a region with some meandering tori. The plot in the right is the rotation number of the invariant curves and the peak, with a pink arrow, corresponds to an extreme of the rotation number, which is associated with a meandering torus of the pink region. Figures (4,5,6) are authorized reproductions:"© IOP Publishing. Reproduced by permission of IOP Publishing. All rights reserved", of the original work: Martins C G L, Egydio de Carvalho R, Caldas I L and Roberto M 2011 J. Phys. A **44** 045102.

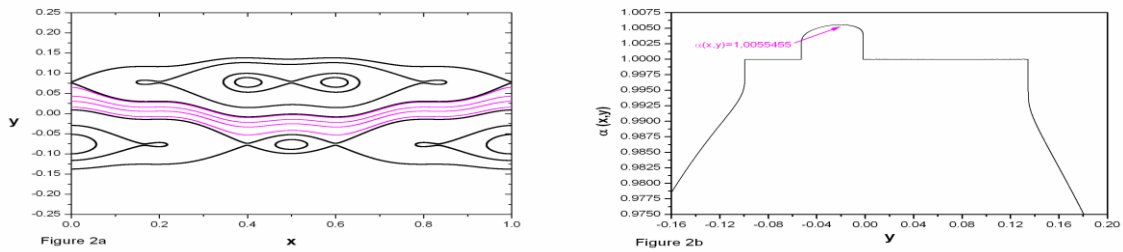

Figure 4: A meandering region (pink) is shown before the overlap of the isochronous resonances and the rotation numbers of the phase space in the left. The extreme of the rotation number corresponds to the shearless torus.

The parameter b controls the amplitude of the sinusoidal perturbations and allows the resonances overlapping. In figure (5) we chose b = 0.005. The coloured regions correspond to three different regions with meandering tori which are visualised through the three minima in the rotation number plot. The reader should note that for the current set of parameters the system seems to be integrable because the chaotic layers are so thin for the scale of the plots.

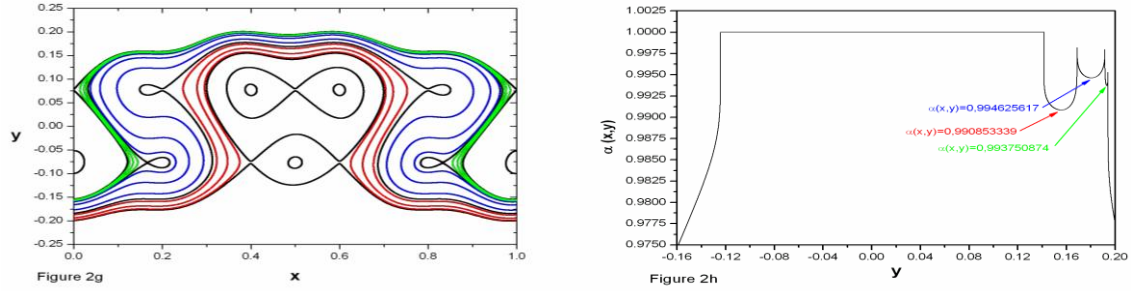

Figure 5: Three meandering regions are shown after the overlap of the isochronous resonances. There are three shearless curves each one associated with a minimum of the rotation number.

In figure (6) we increase the value of the perturbation parameter, now b = 0.043 and a wide chaotic region can be seen. The blue and green regions have been broken and the corresponding orbits became chaotic. The survivor red region contains the more robust meandering torus, called shearless curve,

and when we look for its rotation number we observe that the red shearless torus has the lowest value among the three minima.

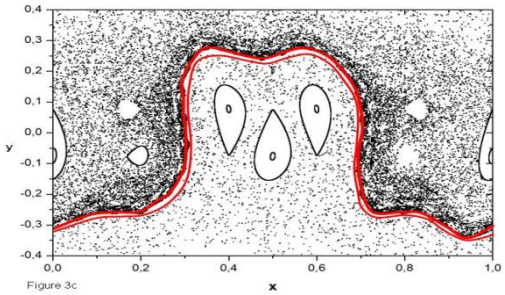

Figure 6: The destruction of the resonance structures and of the meandering regions is obtained increasing the parameter b. The more robust shearless, that has been survived to the effect of the perturbation, corresponds to the lowest minima of the rotation number.

5. Final remarks

We presented some fundamental tools of non-linear dynamics which are typical of Hamiltonian systems. We showed the isochronous resonances, which occur only in non-twist systems, governed by a Hamiltonian or by a map, robust tori which correspond to transport barriers for the dynamics and the meandering tori. These appear in the regions of isochronous resonances, as before as after the reconnection process. Even though the robust tori can occur as in twist as in non-twist systems, we presented their effects in a system with isochronous resonances. The movement of the robust tori among the island chains leads to two different topological rearrangements, one with the similar fixed points aligned and another one with the fixed points defocused. The meandering tori appear when the rotation number presents an extreme and we showed that the more robust of them has the minor minimum value. And to conclude we state that the isochronous resonances are actually part of the foundations of the non-linear theory.

Acknowledgements: We thank the Brazilian scientific agency, FAPESP, for financial support through the process 2010/ 20276-2.

References

[1] Chierchia L and Mather J N 2010 Scholarpedia **5**(9) 2123.
[2] Mackay R S and Meiss J D 1987 *Hamiltonian Dynamical Systems-a reprint selection*, Adam Hilger.
[3] Voyatziz G, Ichtiaroglou S 1999 Int. J. Bifurcation Chaos **9** 849.
[4] Egydio de Carvalho R and Ozorio de Almeida A M 1992 Phys. Lett. A **162** 457.
[5] Howard J E and Hohs S M 1984 Phys. Rev. E **29** 418.
[6] Delshams A and de la Llave R 2000 SIAM J. Math. Anal. **31** 1235.
[7] Ozorio de Almeida A M 1987 *Sistemas Hamiltonianos: Caos e Quantização* Editora da Unicamp.
[8] Egydio de Carvalho R 1993 Nonlinearity **6** 973.
[9] Voyatzis G, Meletlidou E and Ichtiaroglou S 2002 Chaos, Sol. Frac. **14** 1179.
[10] Egydio de Carvalho R, Martins, C GL and Favaro G M 2009 Braz. J. Phys. **39** 606.
[11] Egydio de Carvalho R and Favaro G M 2005 Physica A **350** 173.
[12] Martins C G L, Egydio de Carvalho R, Caldas I L, Roberto M 2011 Physica A **390** 957.
[13] del-Castillo-Negrete D, Greene J M and Morrison P J 1996 Physica D **91** 1.
[14] Wurm A, Apte A and Morrison P J 2004 Braz. J. Phys.**34** 1700.
[15] Szezech Jr J D, Caldas I L, Lopes S R, Viana R L and Morrison P J 2009 Chaos **19** 043108.
[16] del-Castillo-Negrete D and Morrison J P 1993 Phys. Fluids A **5** 948.
[17] Wurm A, Apte A, Fuchss K and Morrison J P 2005 Chaos **15** 023108.
[18] Martins C G L, Egydio de Carvalho R, Caldas I L and Roberto M 2011 J. Phys. A **44** 045102.